Supplementary Information

Novel inorganic solid state ion conductor for rechargeable Mg battery

S.Higashi, K.Miwa, M.Aoki, K.Takechi

1 Synthesys of $Mg(BH_4)(NH_2)$ and characterizations

$Mg(BH_4)_2$ was purchased from Sigma-Aldrich and $Mg(BH_4)(NH_2)$ was synthesized via a mechanochemical reaction promoted by grinding in a planetary ball mill and subsequent annealing of a mixture of $Mg(BH_4)_2$ and $Mg(NH_2)_2$ (50:50 mol%). Details of sample characterizations by XRD and Raman spectroscopy are described in supplementary information. Further details of the synthesis of $Mg(BH_4)(NH_2)$ can be found elsewhere [1]. The sample powders thus obtained were cold-pressed into pellets 10 mm in diameter and 0.5 mm thick in an Ar filled glove box at room temperature.

1.1 Impedance measurements

Impedance measurements were performed using a chemical impedance meter (3532-80,HIOKI) over the range of 4 Hz to 1 MHz. During these measurements, samples were held at constant temperature in a constant-temperature chamber (SH-241,ESPEC). Biologic (VMP3) and ASKA charge-discharge systems (ACD-M00-5N) were used for cyclic voltammogram and OCVs measurements.

1.2 XRD spectrum of $Mg(BH_4)(NH_2)$

XRD profile of obtained crystalline $Mg(BH_4)(NH_2)$ is shown in Fig S1. A RINT-2200 (RIGAKU) diffractometer with Cu K radiation was used for XRD measurements. Sample powder was mounted in an aluminum holder and secured with adhesive tape in an Ar glove box.

1.3 Raman Spectra for Magnesium borohydride ($Mg(BH_4)_2$), Magnesium Amide ($Mg(NH_2)_2$) and $Mg(BH_4)(NH_2)$

Raman Spectrum of $Mg(BH_4)_2$, $Mg(NH_2)_2$ and $Mg(BH_4)(NH_2)$ are shown in Fig S2. B-H [2][3], and N-H stretching [4, 5] mode can be clearly seen in $Mg(BH_4)(NH_2)$ raman spectrum. Raman spectroscopy (NRS-3300, JASCO) measurements were carried out under the Ar gas atmosphere.

2 Mg depth profile analysis by Glow Discharge Optical Emission Spectroscopy (GD-OES)

Mg depth profiles were acquired by GD-OES(GD-Profiler2, HORIBA). We applied a voltage sweep from 0 to -1V (vs. Mg R.E) to the Pt electrode with sweeping rate of 1mv/sec at 150°C. Upon reaching a bias of -1 V, the external bias was abruptly removed and then, test cell was unpacked and Pt electrode was pealed off in the Ar gas glove box. Spectrum was taken from $Mg(BH_4)(NH_2)$ surface towards Mg electrode side. We also measured the profile for pristine $Pt/Mg(BH_4)(NH_2)/Mg$ test cell for obtaining a comparable reference data. Except that the latter cell (the pristine cell) has not been experience the voltage sweep, every procedure is the same as the voltage applied test cell. GD-OES measurements were carried out under the Ar gas atmosphere.

3 OCVs measurements for Mg-sulfide electrochemical test cells

The Mg-S test cell consisted of a 0.1 mm thick Mg metal plate (99.9 % Nilaco) on which 40 mg $Mg(BH_4)(NH_2)$ was cold-pressed to a thickness of 0.5 mm, stacked together with a pellet made of cold-pressed sulfur (99.99 %, Koujyundo Chemical) and Ketjen Black (85 %, Mitsubishi Chemical, ECP-600JD) (70:30 wt%), as shown in the inset to Fig. S4(b). For the Mg-FeS battery, a cold-pressed FeS (99.9 %, Aldrich) pellet was used as the cathode. Platinum plates were employed as current collectors. All components, current collectors, electrodes and solid electrolytes were ϕ10 mm in diameter and were mounted in air-proof cells filled with Ar gas. All measurements were carried out at 150 °C. The OCVs obtained were approximately 1.4, 1.2 and 1.3 V for Mg-S, Mg-FeS and Mg-Ag_2S, respectively, which is in good agreement with voltage values predicted by DFT calculations (Table. 1).

4 *Ab-initio* molecular dynamics simulations

Theoretical calculations were performed using the ultra-soft pseudo potential method based on density functional theory [6, 7]. The generalized gradient approximation was adopted for the exchange-correlation function [8] and the cutoff energy was set to 15 hartrees for the pseudo wave functions and 120 hartrees for the charge density. The k-point grids used in Brillouin zone integration were generated so as to make the edge lengths of the grid elements as close to the target value of 0.08 $bohr^{-1}$ as possible. Theoretical working voltages for the Mg battery systems were estimated simply by calculating the total energy difference between reactants and products.

The Mg diffusion in $Mg(BH_4)(NH_2)$ has been investigated using *ab-initio* molecular dynamics simulations based on density functional theory [6, 7]. We adopt the meta-dynamics [9] to enhance the motion of an Mg atom for which a history-dependent potential is introduced:

$$V = \sum_{i}^{n-1} V_0 \exp\Big[-\Big|\frac{\mathbf{R}_n - \mathbf{R}_i}{W}\Big|^2\Big],$$

where R_i denotes the atomic position at ith time step, and potential parameters V_0 and W are set to be 1×10^{-4} hartree and 0.3 bohr, respectively. A super cell containing 288 atoms (32 formula units) is used. Temperature is constrained to be 423 K and a time step is 0.73 fs. After thermal equilibration of 2000 steps, the potential V is switched on and the meta-dynamics is performed for 30000 steps. The obtained trajectories are given in Fig S5. A target Mg atom which is affected by the potential V shows hopping to an interstitial site across the NH_2 layer. Figure S6 depicts the contour plot of the potential V around the target Mg atom, which is expect to be a good measure of the potential energy surface for Mg motion. From the highest peak of V, the energy barrier for Mg hopping to an interstitial site is guessed as about 0.6 eV. We also repeat the simulation with two target atoms. Mg hopping across the NH_2 layer only occurs and that across the BH_4 layer is never observed. For the latter motion, the nudged elastic band calculation [10] gives the energy barrier more than 4 eV. Though we have not determined the Mg migration path yet, these results suggest that the Mg diffusion channels are two-dimensional perpendicular to the c axis. The Mg atom can move to the interstitial site (namely, the formation of a Frenkel pair) with a relatively small energy cost, which will be a precursor state for the Mg migration.

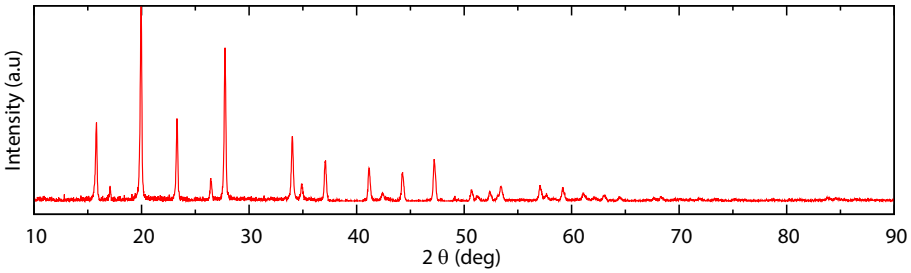

Figure S1: XRD profile of obtained crystalline $Mg(BH_4)(NH_2)$.

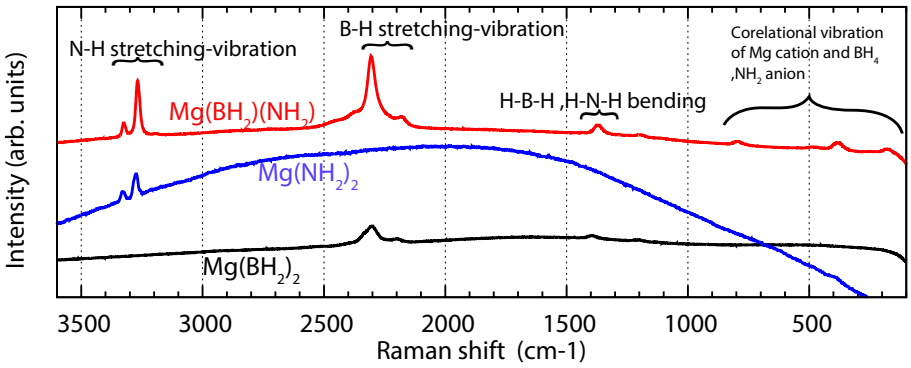

Figure S2: Raman Spectrum of $Mg(BH_4)_2$, $Mg(NH_2)_2$ and $Mg(BH_4)(NH_2)$.

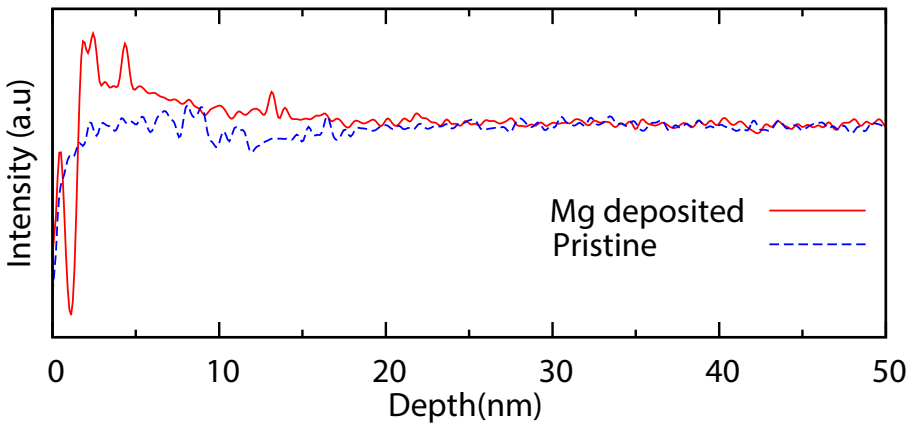

Figure S3: Mg depth profile acquired by GD-OES).

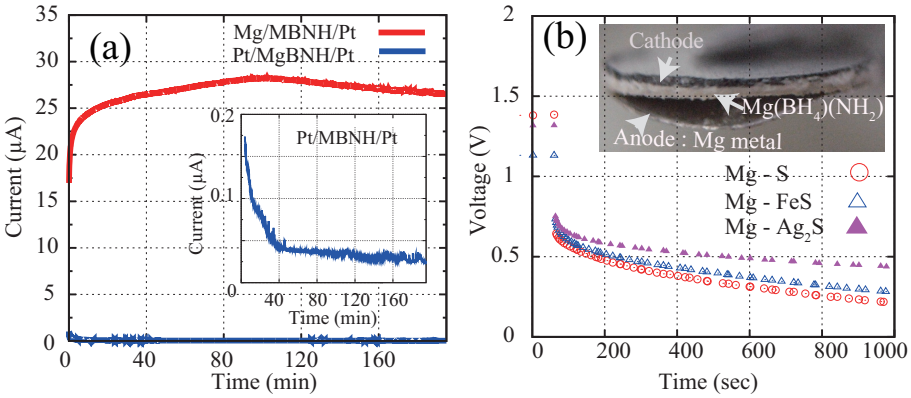

Figure S4: (a) Typical current response for $Pt/Mg(BH_4)(NH_2)/Pt$ and $Mg/Mg(BH_4)(NH_2)/Pt$. Inset shows the magnified profile. (b) Discharge curves for Mg-S, Mg-FeS and Mg-Ag_2S electrochemical test cells using $Mg(BH_4)(NH_2)$ as the electrolyte at 150°C. Inset shows a photo of the battery. Discharge current density is 0.5 $\mu A/cm^2$. For illustrative purposes, the Mg metal has been partially stripped off.

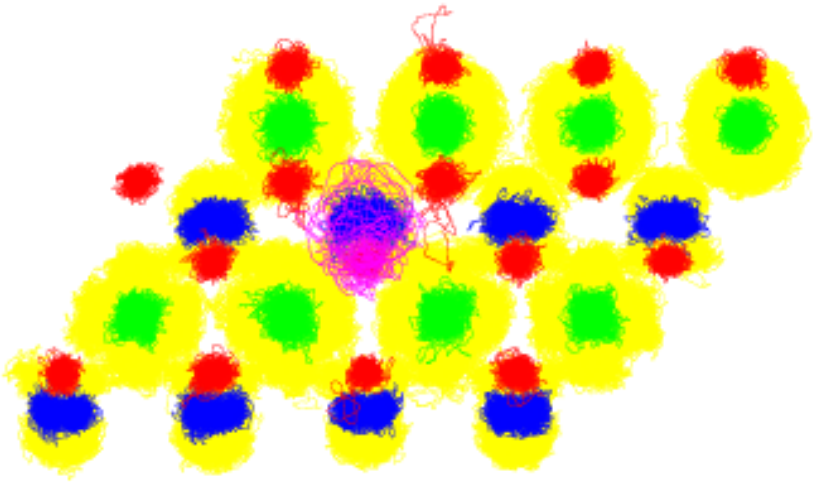

Figure S5: Trajectories in the meta-dynamics simulation. A purple line shows the target Mg atom and red lines show other Mg atoms. Green, blue, and yellow lines indicate B, N, and H atoms, respectively.

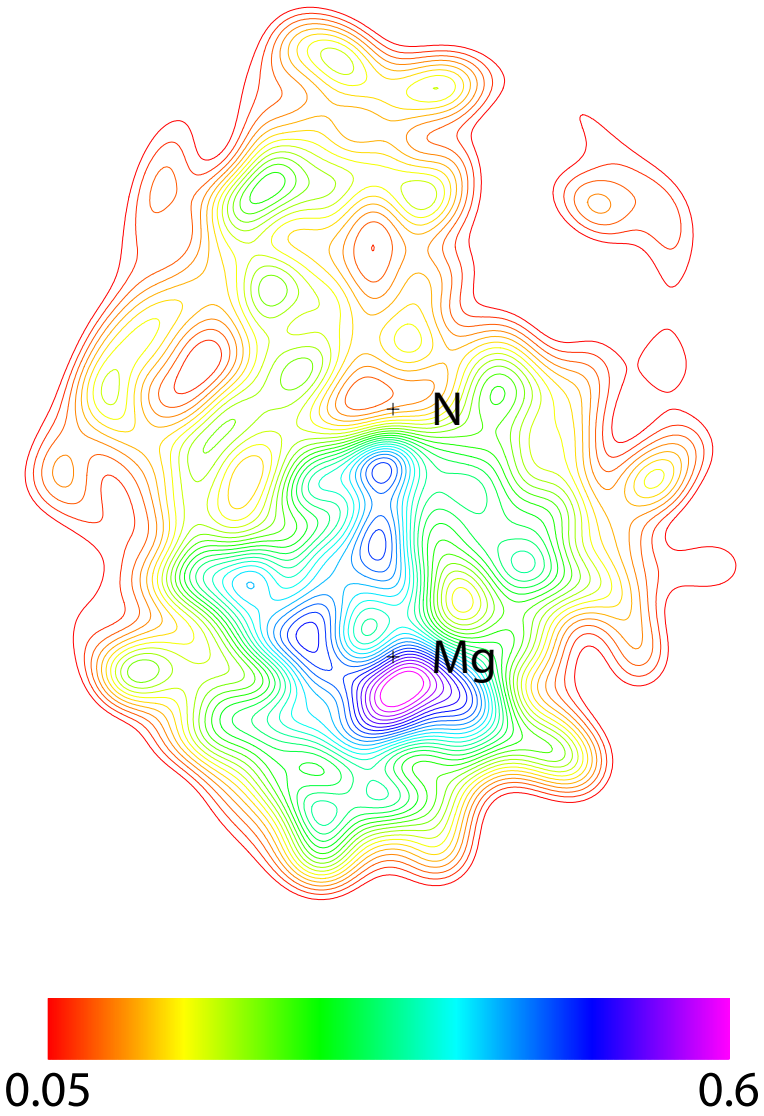

Figure S6: Contour plot of the history-dependent potential V. The contour space is 0.05 eV. The cross marks indicate the equilibrium atomic position for the target Mg and the neighboring N (projected on the plane) atoms.

References

[1] T. Noritake, K. Miwa, M. Aoki, M. Matsumoto, S. ichi Towata, H.-W. Li and S. ichi Orimo, International Journal of Hydrogen Energy, **38**, 9978 (2013).

[2] Florian Gebert, Britta Willenberg, Michiel J. van Setten, Elisa G. Bardaji, Eva Roehm, Maximilian Fichtnerb and Joachim Schoenesa , J. Raman Spectrosc. **42**, 1796 (2011).

[3] K. Miwa, N. Ohba, S. Towata, Y. Nakamori and S. Orimo Phys. Rev. B.**71**, 195109 (2005).

[4] K. Miwa, N. Ohba, S. Towata, Y. Nakamori and S. Orimo Phys. Rev. B.**69**, 245120 (2004).

[5] A. Michigoe, T. Hasegawa, N. Ogita, T. Ichikawa, Y. Kojima , S. Isobe and M. Udagawa, J. Phys. Soc. Jpn. **81** 094603 (2012)

[6] P. Hohenberg and W. Kohn, Phys. Rev. **136**, B864 (1964).

[7] W. Kohn and L. J. Sham, Phys. Rev. **140**, A1133 (1965).

[8] D. Vanderbilt, Phys. Rev. B.**41**, 7892 (1990).

[9] M. Iannuzzi, A. Laio, and M. Parrinello, Phys. Rev. Lett. **90**, 238302 (2003).

[10] G. Henkelman and H. J'ønsson, J. Chem. Phys. **113**, 9978 (2000).